International Journal of Nanomedicine

Dovepress
open access to scientific and medical research

Open Access Full Text Article

ORIGINAL RESEARCH

Rapamycin Liposomes Combined with 5-Fluorouracil Inhibits Angiogenesis and Tumor Growth of APC $^{(Min/+)}$ Mice and AOM/DSS-Induced Colorectal Cancer Mice

Xiao-Min Liu[1,*], Wen-Ting Zhu[1,*], Meng-Lei Jia[1], Yu-Ting Li[1], Ye Hong[1], Zhong-Qiu Liu[2], Peng-Ke Yan[1]

[1]Department of Pharmacy, Biomedicine Research Center, Guangdong Provincial Key Laboratory of Major Obstetric Diseases, The Third Affiliated Hospital of Guangzhou Medical University, Guangzhou, People's Republic of China; [2]Joint Laboratory for Translational Cancer Research of Chinese Medicine of the Ministry of Education of the People's Republic of China, Guangzhou University of Chinese Medicine, Guangzhou, People's Republic of China

*These authors contributed equally to this work

Correspondence: Zhong-Qiu Liu, Joint Laboratory for Translational Cancer Research of Chinese Medicine of the Ministry of Education of the People's Republic of China, Guangzhou University of Chinese Medicine, Guangzhou, People's Republic of China, Email liuzq@gzucm.edu.cn; Peng-Ke Yan, Department of Pharmacy, Biomedicine Research Center, Guangdong Provincial Key Laboratory of Major Obstetric Diseases, The Third Affiliated Hospital of Guangzhou Medical University, Guangzhou, People's Republic of China, Email gysyypk@126.com

Background: Transgenic C57BL/6-APC$^{(Min/+)}$ spontaneous cancer mouse model and the Azoxymethane (AOM)/Dextran Sulfate Sodium (DSS) chemically induced orthotopic colorectal cancer mouse model represented distinct pathogenesis of colorectal cancers. Our previous study revealed that the combination of Rapamycin liposomes (Rapa/Lps) and 5-Fluorouracil (5-FU) has anti-colorectal cancer effects. However, the therapeutic efficacy of Rapa/Lps and 5-FU in other colorectal cancer mice models is yet to be thoroughly explored. The purpose of this study was to investigate the anti-tumor effect of Rapa/Lps combined with 5-FU in vivo and in vitro.

Methods: In this study, we evaluated the effect of Rapa/Lps and 5-FU on APC $^{(Min/+)}$ mice and AOM/DSS-induced colorectal cancer mice. The small intestine, colorectum, serum, and plasma of mice in each group were collected following sacrifice to record the number of tumors. HE staining was utilized for observing pathological damage to intestine tissues. Tube formation assay, Transwell assay, wound healing assay, Western Blot were used to explore the anti-angiogenesis effect of drugs in HUVECs.

Results: As expected, Rapa/Lps and 5-FU significantly suppressed tumor formation, decreased the number of tumors, and tumor load both in two mouse models, and had no influence on mouse weight. Mechanically, the anti-tumor effect of the drug also was associated in inhibiting angiogenesis and proliferation. Furthermore, we found that Rapa/Lps obviously inhibited HUVECs tube formation and migration.

Conclusion: Altogether, we revealed the Rapa/Lps synergism with 5-FU decreased colon and small intestinal tumorigenesis in AOM/DSS-treated and APC $^{(Min/+)}$ mice, respectively, and correlated with anti-angiogenesis.

Keywords: rapamycin liposomes, 5-fluorouracil, angiogenesis, APC $^{(Min/+)}$ mice, AOM/DSS, colorectal cancer

Introduction

Colorectal Cancer (CRC) is the third leading cause of cancer death in both men and women.[1] Accumulating studies show that inflammatory factors, immune cells, genetic factors, and intestinal flora contribute to the occurrence, development, and metastasis of CRC.[2] APC $^{(Min/+)}$ mice can spontaneously generate a large number of intestinal multiple adenomas, which is an excellent animal model for familial adenomatous polyposis (FAP) research.[3] The combination of azoxymethane (AOM) and dextran sodium sulfate (DSS) can induce colitis-associated cancer mice model.[4]

The clinical treatment of colorectal cancer includes surgery, chemotherapy, and radiotherapy.[5] 5-Fluorouracil (5-FU) was the first-line basic chemotherapy agent for colorectal cancer, but it also has disadvantages such as high toxic side effects and

Received: 26 May 2022
Accepted: 26 September 2022
Published: 27 October 2022

has easy drug resistance.[6] The combination of different drugs is routinely used in clinical practice for the treatment of cancer. It not only reduces the dosage of single drugs and provides a synergistic effect, but also may improve the toxic side effects of the drugs.[7] For example, ethanolic extracts of Thai noni juice (TNJ) products in combination with 5-FU enhanced the anti-cholangiocarcinoma activity in mouse KKU-100 xenograft model through apoptosis induction and reduced toxicity of 5-FU.[8] In another study, metformin synergized with 5-FU to inhibit CRC proliferation and metastasis.[9]

Rapamycin, a classic mTOR inhibitor, has recently been approved as an anti-cancer therapy in a variety of preclinical models for the treatment of renal cell carcinoma, pancreatic cancer, and colorectal cancer. However, rapamycin's clinical use has been hampered by its poor water solubility, low bioavailability, and instability in circulation.[10] Our previous study developed a rapamycin liposomes system (abbreviated to, Rapa/Lps) to address this problem, and we discovered that Rapa/Lps effectively suppressed the tumor growth in the HCT-116 xenograft model.[11] However, xenograft models were limited by the lack of broad molecular transformations like human tumors, and their growth rates were considerably faster than primary tumors.[12] As a result, the xenograft was unable to provide a clear indication of the potential effects of rapamycin liposomes with 5-FU.

Hence, our present study investigated the effects and the underlying mechanism of Rapa/Lps combined with 5-FU on tumor formation in APC $^{(Min/+)}$ and AOM/DSS mouse models. Firstly, we evaluated the effects of the combination of Rapa/Lps and 5-FU on the tumor development in APC$^{(Min/+)}$ and AOM/DSS-treated mice. Then, we estimated the combination effects on the proliferation, migration, and angiogenesis in vitro and in vivo.

Materials and Method

Materials and Animals

Materials

Dextran Sulfate Sodium (DSS, meilunbio, Dalian, China), Azomethane (AOM, Sigma-Aldrich, USA), Ki67, CD31 (1:100, Servicebio, Wuhan, China), SP Rabbit & Mouse HRP Kit (DAB, Cwbio, Jiangsu, China). DAB Kit (1:20, Cwbio, Jiangsu, China), 5-Fluorouracil (Meilunbio, Dalian, China).

Rapamycin Liposomes (Rapa/Lps) were developed according to Chen et al. The particle size of Rapa/Lps was 100 ±5.5 nm, the PDI was 0.125–0.25, and the zeta potential was nearly neutral.

Cell Culture

The Human umbilical vein endothelial cells (HUVECs) were purchased from Procell Corporation (Procell, Wuhan, China). HUVECs were cultured in High glucose DMEM medium (Corning) supplemented with 10% fetal bovine serum (FBS, Excel, Uruguay).100 U/mL of penicillin and 100 mg/mL of streptomycin (Gibco, USA). All cells were cultured in a humidified incubator at 37°C in 5% CO2.

Animal

Male C57BL/6J mice (16–20 g, aged 6–8 weeks) were purchased from Zhuhai BesTest Bio-Tech Co, Ltd (Zhuhai, China, SCXK20200051).

APC $^{(Min/+)}$ mice were gifted by Zhong-qiu Liu professor (Guangzhou University of Traditional Chinese Medicine International Institute for Traditional Chinese Medicine). APC $^{(Min/+)}$ mice were genotyped according to the supplier's instructions by using allele-specific PCR analysis of tail DNA. The genotypes were determined using primers by PCR (Wild-type: GCC ATC CCT TCA CGT TAG, APC min: TTC TGA GAA AGA CAG AAG TTA, Common antisense: TTC CAC TTT GGC ATA AGG C). Then, we evaluated PCR products by agarose gel electrophoresis.

All mice were housed under standard conditions (12:12 h light/dark cycle at 25±2°C and 40-70% humidity) in specific pathogen-free (SPF) conditions, with ad libitum access to food and water. All animal studies were performed in accordance with the legal mandates and national guidelines for the care and maintenance of laboratory animals. The Laboratory Animal Ethics Committee of the Third Affiliated Hospital of Guangzhou Medical University approved all experimental protocols.

Animal Experiment

The AOM/DSS Inflammation-Associated Colon Carcinogenesis Model

As previously described,[13] the inflammation-associated cancer was induced in C57BL/6 mice using AOM and DSS. Summarily, mice received a single intraperitoneal injection of AOM (12.5 mg/kg, i.p.) after intervention feeding. After one week, mice were exposed to 2.5%DSS (wt/vol) for 7 days, followed by regular water drinking for 14 days. This cycle was then repeated three times.

One week after the last DSS drinking, mice were randomly divided into four groups (n = 6), saline, Rapa/Lps (2 mg/kg), 5-FU (30 mg/kg), Rapa/Lps+5-FU. Mice were treated with Rapa/Lps through tail vein injection twice a week, and 5-FU through intraperitoneal injection twice a week. The duration for Rapa/Lps and 5-FU administration was specified by Chen et al[11] and Khondee et al[14], We monitored the weight twice a week for a month during the experiment.

The APC $^{(Min/+)}$ Genetic Cancer Susceptibility Model

The 6–8 weeks APC $^{(Min/+)}$ mice were fed a high fat diet (HFD) diet. After 8 weeks, mice were randomly divided into four groups (n = 9), saline, Rapa/Lps (2 mg/kg), 5-FU (30 mg/kg), and Rapa/Lps+5-FU.

At the end of the experiment, all mice were sacrificed by cervical dislocation and blood samples were collected to detect blood routine and biochemical indexes. The colorectal tissues were obtained and used for the hematological assay.

Blood Routine Index and Biochemistry Index

A blood biochemistry index, namely Red Blood Cell (RBC), Hematocrit (HCT), Hemoglobin (Hb), and a blood routine index, namely Aspartate aminotransferase (ALT), Alanine aminotransferase (AST), Creatinine (Cre) were detected by the Clinical Laboratory of the Third Affiliated Hospital of Guangzhou Medical University.

Cellular Uptake Assay

Cellular uptake of liposomes was visualized by using a fluorescence confocal microscope (Nikon, A1R+N-STORM, Tokyo, Japan) using coumarin 6 (Cou-6) as the fluorescent probe. Coumarin 6 liposomes (Cou-6/Lps) were prepared by the method reported in our previous publication.[11] HUVECs (5×10^4 cells/well) were grown in complete media on the confocal dish. Cells were treated with free Cou-6 and Cou-6/Lps at a concentration of 10 μg/mL for 1 and 4 h in serum-free media. Then, cells were fixed with 4% paraformaldehyde for 15 min at room temperature. The cell culture plate was washed thoroughly with PBS and stained with DAPI at room temperature, the cell culture plate was observed with the confocal microscope.

Cell Cytotoxicity Assay

2×10^3 cells/well of HUVECs were seeded in a 96-well plate until adherent. Afterward, the cells were incubated with free Rapa, Rapa liposomes, and 5-FU alone or Rapa/Lps combined with 5-FU, respectively. MTT assay (Solar, Beijing, China) was used to detect cell proliferation activity. Absorbance was then measured by the microplate reader at 490 nm (Elx-808, Bio-Tex, Richmond, CA). The 50% concentration of inhibition (IC_{50}) was obtained by SPSS 26.0 software.

Tube Formation Assay

The matrix gel was diluted by serum-free DMEM culture medium (1:2), adding 400 μL of cold matrix gel in a 24-well plate, and incubated at 37 °C overnight. HUVECs (4×10^4 cells) were seeded onto the gelled basement. The cells were treated with Rapa/Lps (4 μg/mL) and 5-FU (12.5 μM) alone or in combination for 4–6 h. Tube-like structures were examined with a Nikon microscope (Nikon, Tokyo, Japan).

Transwellassay

HUVECs were suspended with the serum-free medium that contains 4 μg/mL Rapa/Lps and 12.5 μM 5-FU alone or in combination and transferred into the upper wells of 24-well transwell chambers (BD, Bioscience, USA) at a density of 3×10^5/well. The lower chambers were filled with medium containing 10% FBS. After 24 h incubation, the cells in the upper wells were removed and the cells lower were fixed with 4% paraformaldehyde and dyed with 1% crystalline violet

(Leagene, Beijing, China). Images were captured using a Nikon microscope. Cell counts of translocation were analyzed using Image J.

Wound Healing Assay

5×10^5/well of HUVECs were seeded on 6-well plates. 12 h before treatment, the medium was replaced with that serum-free. Three straight lines were drawn in the middle of each well using a 200 μL tip. The cells were treated with 4 μg/mL Rapa/Lps and 12.5 μM 5-FU supplemented with a 2% FBS culture medium. Images were captured at 24 h using a Nikon microscope. The distance of cell migration was analyzed using a Nikon microscope.

Western Blot

The HUVECs were treated with Rapa/Lps (4 μg/mL) and 5-FU (12.5 μM) alone or combination for 48 h. The protein sample was extracted by RIPA lysis buffer containing protease and phosphatase inhibitor cocktail at 4°C. Then, samples were separated using SDS-PAGE gel and transferred onto the polyvinylidene difluoride (PVDF) membrane, blocked with 5% skim milk (Brofoxx, Germany), and incubated with primary antibody at 4 °C overnight (VEGF, Proteintech, diluted 1:1000, GAPDH, Bioworld, diluted 1:1000). After washing with 0.1%TBST three times, the samples were incubated with a secondary antibody for 1.5 h at room temperature, and ECL illuminating solution (Millipore, USA) was used to observe experimental results. Finally, the data was analyzed by Image J software.

HE Staining

The small intestine of APC $^{(Min/+)}$ mice was obtained, washed with sterile PBS, and fixed with 4% formalin. The whole intestinal mucosa was observed by making Swiss roll and staining with hematoxylin and eosin.

Immunohistochemistry

The tissue sections were deparaffinized in xylene and dehydrated with decreasing concentration of alcohol. Antigen retrieval was incubated with citrate buffer. Then, sections were incubated with the primary antibody in PBS (CD31, Ki67 Servicebio, 1:100) overnight at 4 °C. SP Rabbit & Mouse HRP Kit (DAB) was used, and the sections were incubated with secondary antibody at room temperature for 10 min. After that, DAB solution was added to the sections, developed color for 2~5 min, and terminated in demonized water in time. Cell nuclei were stained using hematoxylin solutions. The image was taken with a Nikon microscope (Nikon EclipseTi, Melville, USA).

Statistical Analysis

The results were expressed as mean ± SEM. Statistical differences were analyzed by one-way ANOVA for multiple comparisons using SPSS/Win 26.0 software (SPSS, Inc., Chicago, IL, USA). Differences were considered significant at $P<0.05$.

Results

The Combination of Rapa/Lps and 5-FU Decreased the Number and Load of Intestinal Tumors in APC $^{(Min/+)}$ Mice

The genotypic map showed that the DNA band of heterozygous APC $^{(Min/+)}$ mice appeared at 600 bp, which were the wild-type APC band, and a mutant DNA band also appeared at 300 bp (Figure 1A). The decreasing of RBC ($P<0.01$), HCT ($P<0.001$), Hb ($P<0.05$), and splenomegaly (Figure 1B and C) were observed in APC $^{(Min/+)}$ mice compared with WT mice. The APC $^{(Min/+)}$ mice appeared with several small intestinal tumors (Figure 1D and I). These results indicated an intestinal carcinogenesis model was successfully established.

Then, we evaluated the anti-tumor effects of treatments Rapa/Lps and 5-FU combination in APC $^{(Min/+)}$ mice. The tumor of APC $^{(Min/+)}$ mice mainly appeared in small intestine. We illustrated the distribution of tumor numbers in the duodenum, jejunum, and ileum in Figure 1E and F, which was determined that all the numbers in the duodenum, jejunum, and ileum were distributed evenly. However, the number of tumors in the Rapa/Lps+5-FU group was

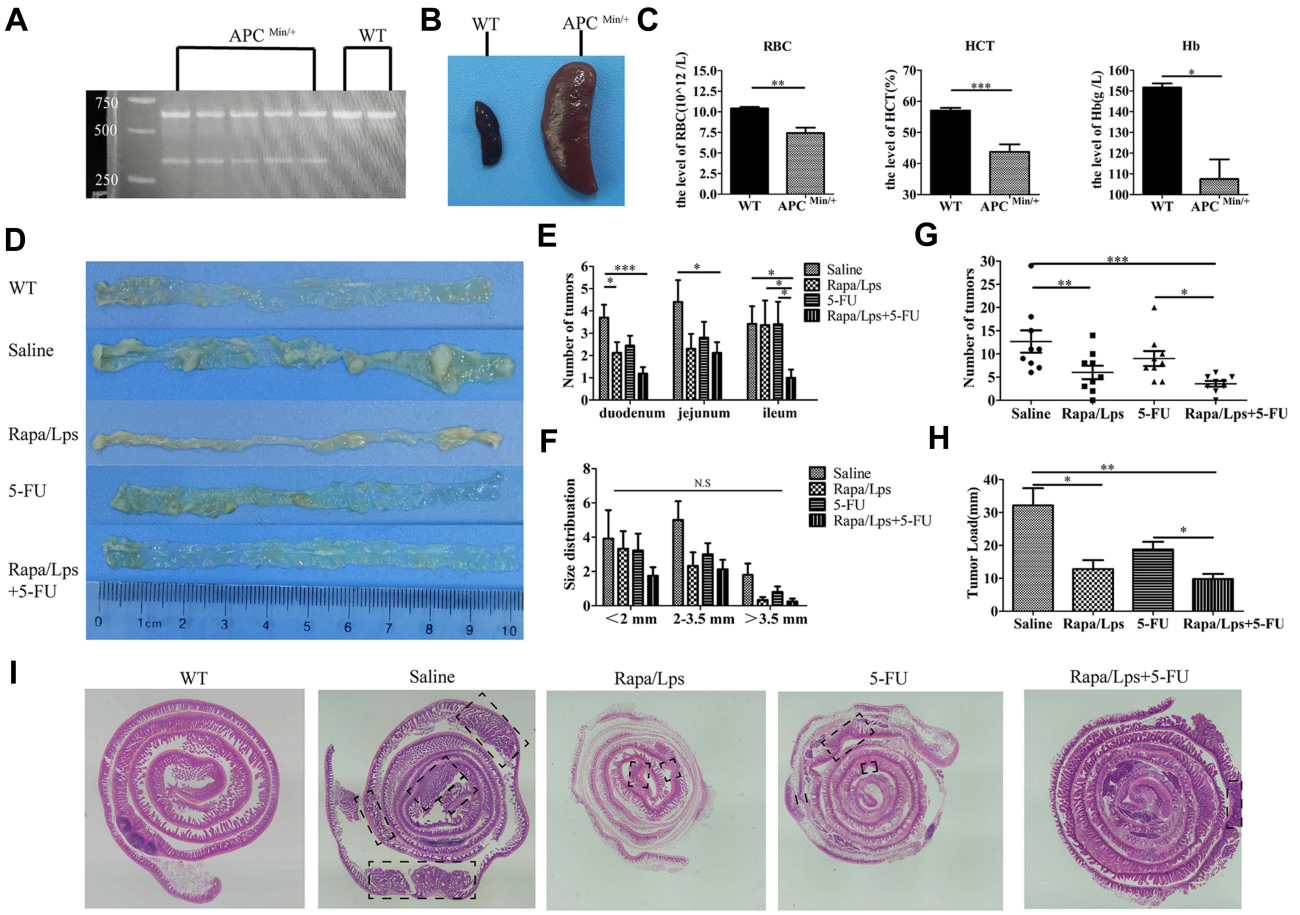

Figure 1 The combination of rapamycin liposomes and 5-FU suppress intestinal adenomas growth in APC$^{(Min/+)}$ mice. (**A**) Agarose gel assay showing the genotyping map of APC$^{(Min/+)}$ and WT mice. (**B**) Schematic illustration of spleen in APC$^{(Min/+)}$ and WT mice. (**C**) The serum level of red blood cell (RBC), hemoglobin (Hb) and hematocrit (HCT) in APC$^{(Min/+)}$ and WT mice. (**D**) Schematic illustration of small intestinal of mice. (**E** and **F**) The distribution profile of adenomas size and the relative distribution of the tumors, expressed as the percentage of tumor in each segment versus total number of tumors between the groups. The quantitative analysis of tumor number (**G**) and tumor load (**H**). (**I**) Representative Swiss roll pictures of small intestines of APC$^{(Min/+)}$ mice, intestinal adenoma is highlighted by arrow. Data are shown as mean ± SEM. *P < 0.05, **P < 0.01, ***P < 0.001.

significantly less in the duodenum, jejunum, and ileum compared with the saline group, respectively. Besides, the macroscopic Swiss roll view of whole small intestines in different drugs treatment reveals the decrease in tumor number (Figure 1I).

Furthermore, we analyzed the tumor number (Figure 1G) and tumor load (Figure 1H) to evaluate the anti-tumor effect of the drug. The tumor number and tumor load in the saline group were (12.67±6.82) and (32.14±14.82 mm), while the tumor number and load were (6.00±4.14, P<0.01) and (12.8±7.70 mm, P<0.05) in Rapa/Lps or (9.0±4.59) and (19.13 ±7.11 mm) in 5-FU. Of note, the tumor number (3.56±1.71, P<0.001) and tumor load (8.13±4.97, P<0.01) in Rapa/Lps +5-FU was obviously reduced compared to saline and 5-FU. Collectively, the therapeutic effect of Rapa/Lps+5-FU was stronger than that of the single group, which was mainly demonstrated by effectively decreasing both tumor number and tumor load.

The Combination ofRapa/Lps and 5-FU Decrease the Formation of Large-Diameter Tumor in AOM/DSS Mouse Model

We successfully constructed the AOM/DSS colitis-induced colorectal cancer mice according to the experimental design in Figure 2A. As shown in Figure 2B and C, the colon length in the model group was shorter than that of WT mice, and a large number of tumors appeared in the rectal, which is consistent with reported by Li et al.[15] Moreover, mice treated with Rapa/Lps and 5-FU alone or in combination displayed favorable responses against colon cancer. The HE staining

indicated that gland structure disorder and inflammatory infiltration appeared in the saline group compared with WT mice; however, inflammatory infiltration was significantly ameliorated in the co-administered group (Figure 2H).

To better illustrate the efficacy of the drug, we analyzed it according to the following four categories of indicators, tumor numbers, tumor load, >3 mm tumor number %, and max tumor diameter. In a comprehensive analysis, we found that tumor numbers in the saline group were not significantly different from those in Rapa/Lps, 5-FU, or Rapa/Lps+5-FU (Figure 2D). The tumor load in Rapa/Lps+5-FU (2.8±1.8 mm) was considerably lower than in saline (9.3±6.5 mm, $P<0.05$), 5-FU (7.3±4.6 mm), Rapa/Lps (4.9±2.1 mm) (Figure 2E). The max tumor diameter and >3 mm tumor numbers in saline were (4.5±1.5 mm) and (77.8±36.9%). After drug treatment, the max tumor diameter and >3 mm tumor number were (2.9±0.5 mm, $P<0.05$) and (22.2±36.9%, $P<0.01$) in Rapa/Lpsor (3.6±1.0 mm) and (25.6±22.9%, $P<0.05$) in 5-FU, which was further reduced to (2.0±1.0 mm, $P<0.01$) and (8.3±18.6%, $P<0.01$) in the Rapa/Lps+5-FU group (Figure 2F and G). Above all, tumor growth was suppressed by the combined treatment of Rapa/Lps and 5-FU, which significantly reduced the formation of large-diameter tumors.

The Combination of Rapa/Lps and 5-FU Suppress the Expression of Ki67 and CD31

As is shown in Figure 3A and C, the number of Ki67 positive cells was decreased in Rapa/Lps+5-FU ($P<0.001$), Rapa/Lps ($P<0.001$), and 5-FU ($P<0.001$) groups. The cell proliferation of tumor cells in Rapa/Lps+5-FU was inhibited.

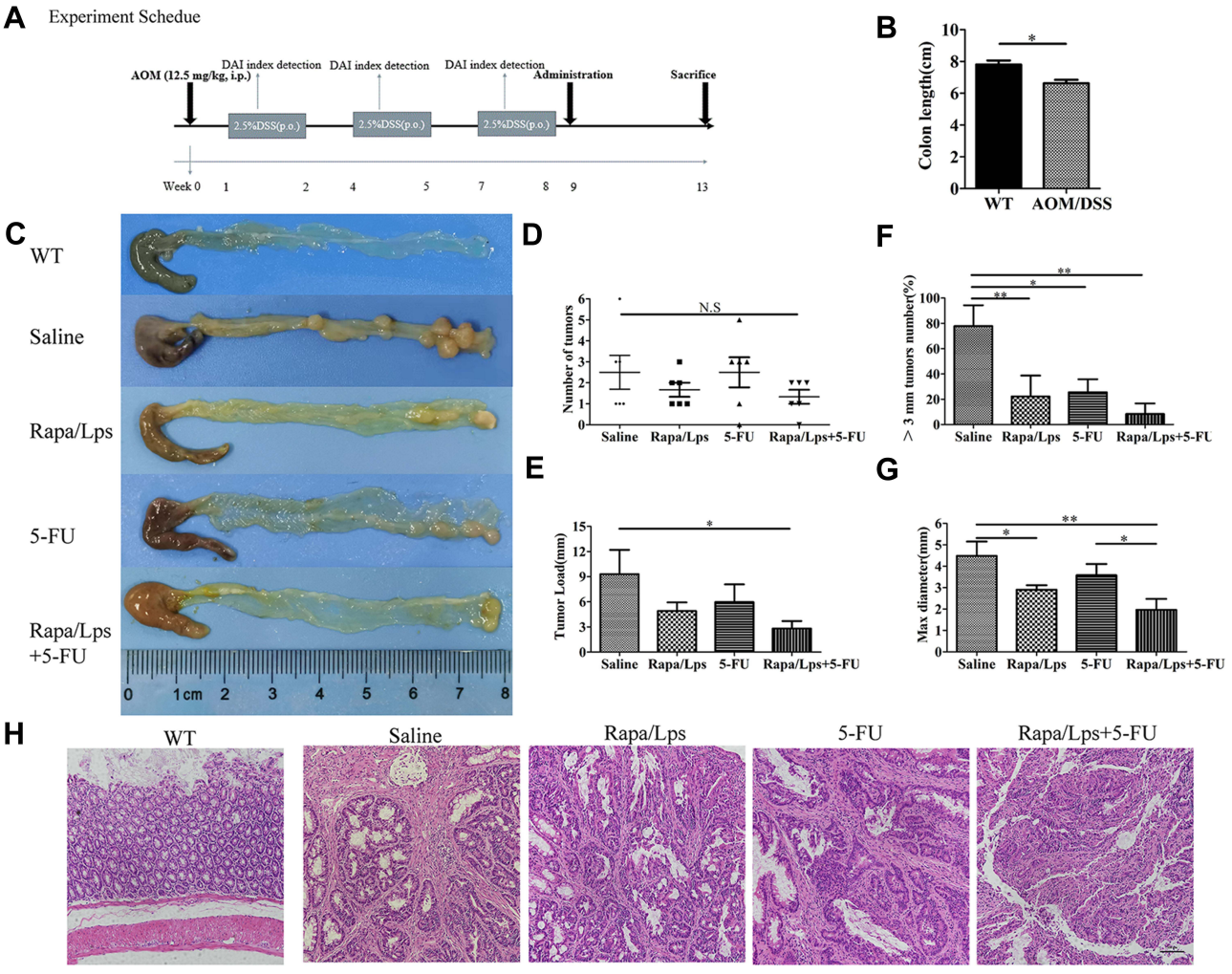

Figure 2 Rapamycin liposomes combined with 5-FU suppresses AOM/DSS-induced colon carcinogenesis. (**A**) Experimental protocol for the establishment of inflammation-associated colon carcinogenesis in C57BL/6 mice induced by AOM/DSS treatment. (**B**) The colon length in WT and AOM/DSS-treated mice. (**C**) Photograph showing colons from experimental groups. The tumor numbers (**D**), and tumor load (**E**) in different drug treatment. (**F**) The quantitative analysis of tumor number which the size >3 mm. (**G**) The quantitative analysis of max diameter. (**H**) HE staining images of colon tissues from experimental groups. Data are shown as mean ± SEM. *P < 0.05, **P < 0.01.

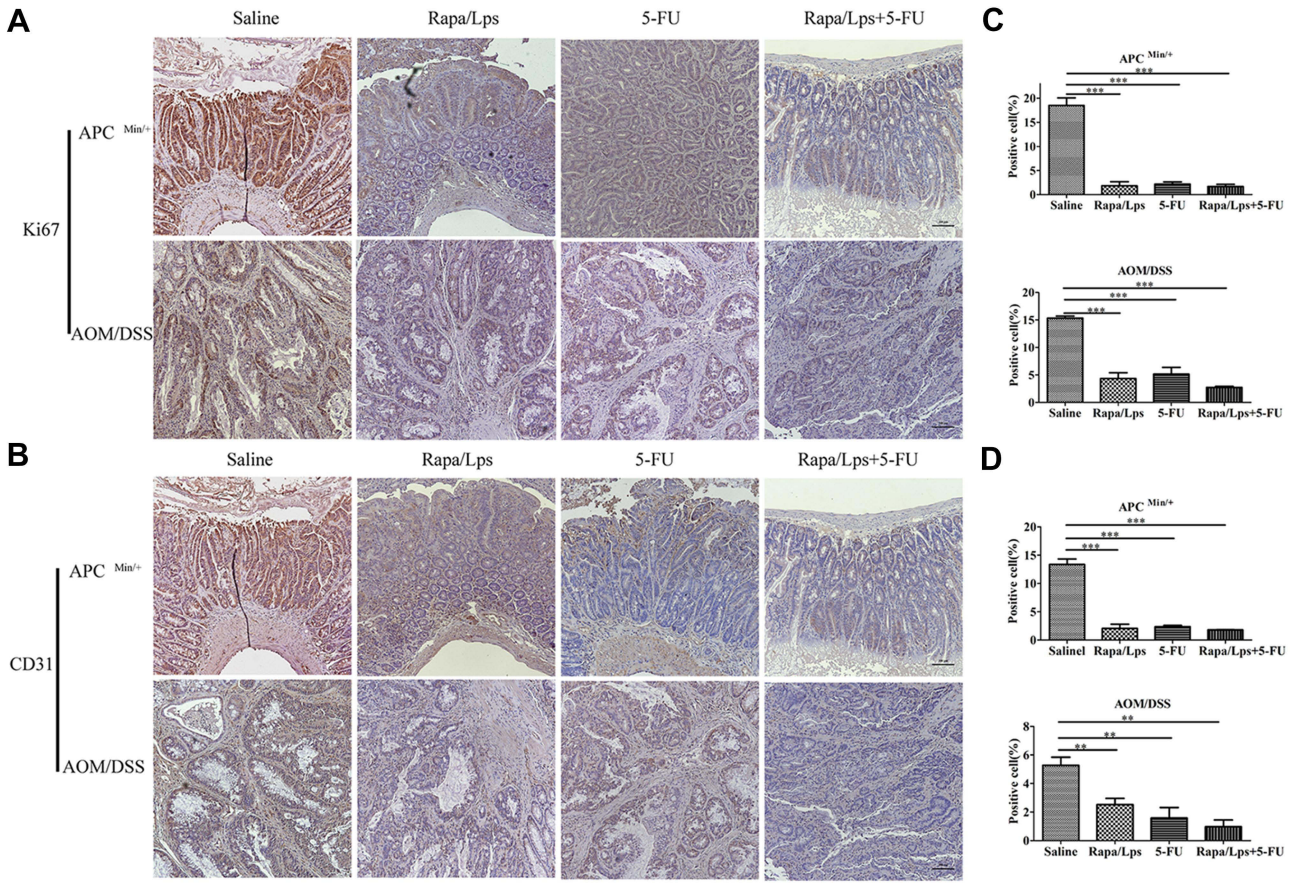

Figure 3 Rapamycin liposomes combined with 5-FU inhibited cell proliferation and angiogenesis in vivo. (**A**) Representative image of Ki67 expression in colon tissue in APC $^{(Min/+)}$ and AOM/DSS colorectal cancer mice. (**B**) Representative image of CD31 expression in colon tissue in APC $^{(Min/+)}$ and AOM/DSS-treated mice. (**C** and **D**) The quantitative analysis of Ki67 and CD31 expression. Data are shown as mean ± SEM. $^{**}P < 0.01$, $^{***}P < 0.001$.

CD31 is an endothelial adhesion factor, which is mainly expressed in immune cells such as vascular endothelial cells, and macrophages. We used CD31 to evaluate the formation of microvessels in colon tissues. As is shown in Figure 3B and D, an evident reduction was observed upon Rapa//Lps combined with 5-FU treatment in two mice models ($P<0.001$). Overall, the combination of Rapa/Lps and 5-FU suppressed tumor growth by inhibiting proliferation and angiogenesis in vivo.

The Safety of Rapa/Lps Combined with 5-FU in Colorectal Cancer Mice

The average weight of the mice in both the APC $^{(Min/+)}$ and AOM/DSS CRC mice remained steady throughout the drug treatment period (Figure 4A). Then, we excessed the impact of drugs on the liver and kidney (Figure 4F). Accordingly, AST, ALT, and Cre levels in serum were unaffected by the drug treatment in two mouse models. HE staining further confirmed that the drug did not adversely affect the liver and kidney functions of the two model mice (Figure 4D and E). Thus, it would appear that these drugs are low-toxic to the liver and kidney.

Furthermore, we found that the spleen of all drug treatments was obviously smaller than in saline group, and the weight of the spleen also became lighter (Figure 4B and C). These results indicated that splenomegaly of APC $^{(Min/+)}$ mice was alleviated after drug treatment.

The Rapa/Lps Inhibited HUVECs Growth in Vitro

To begin with, we used Cou-6 as a fluorescent probe to explore the cell uptake of liposomes with a confocal microscope, as shown in Figure 5A, compared with free Cou-6, the intracellular fluorescence intensity of liposomes was remarkably enhanced, which indicated increasing the uptake of Cou-6 by HUVECs.

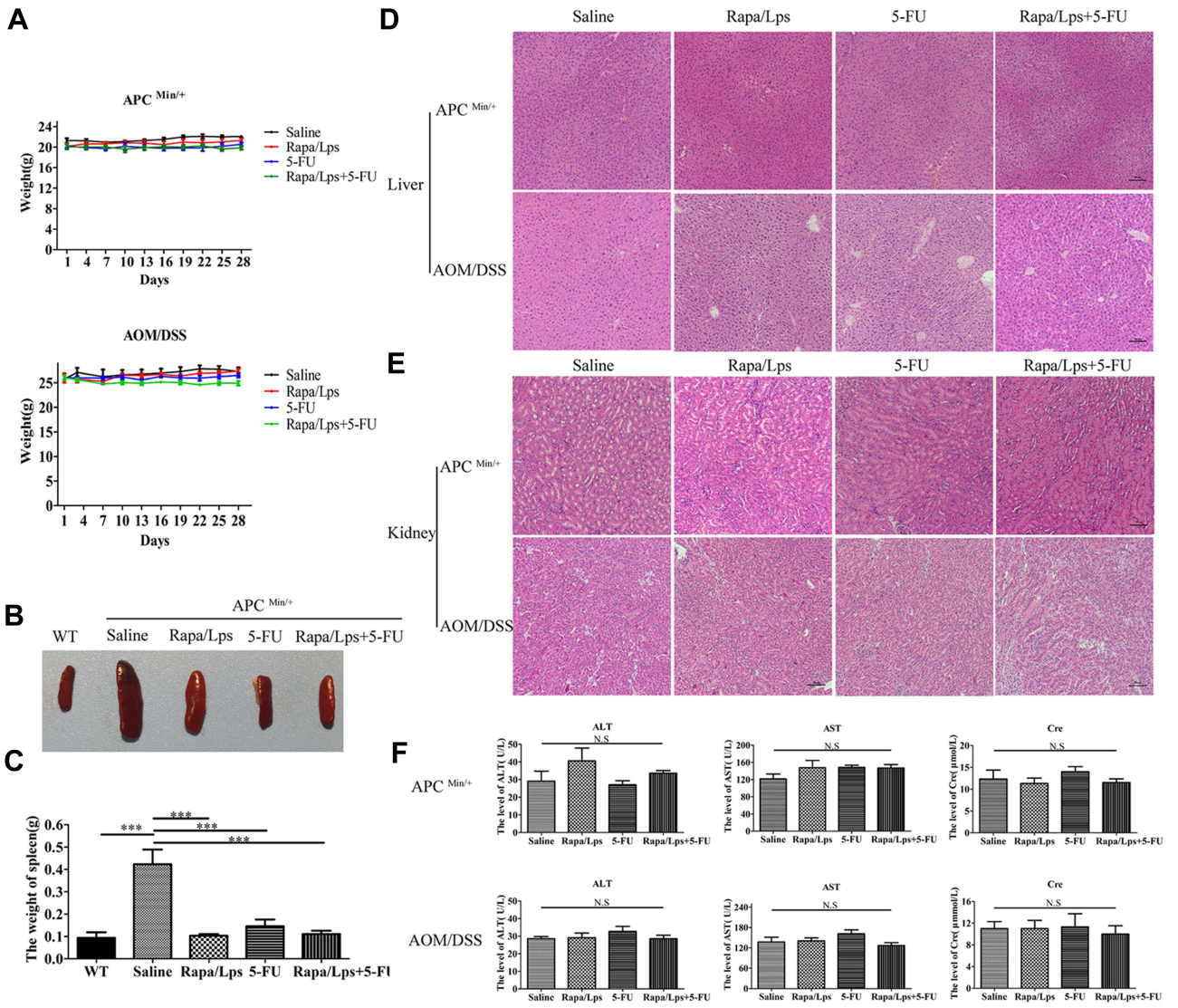

Figure 4 Drugs treatment has no or low impact on body weight, liver and kidney in two mouse model. (**A**) The body weight of APC$^{(Min/+)}$ and AOM/DSS colorectal cancer mice. (**B**) Schematic illustration of spleen with drug treatment in APC $^{(Min/+)}$ and WT mice. (**C**) The weight of spleen in APC$^{(Min/+)}$ and WT mice. (**D** and **E**) Representative HE staining images of liver and kidney in APC$^{(Min/+)}$ and AOM/DSS treated mice. (**F**) The serum level of AST, ALT, Cre in APC$^{(Min/+)}$ and AOM/DSS-induced mice. Data are shown as mean ± SEM. ***$P < 0.001$.

Additionally, we also found that the proliferation of HUVECs was significantly inhibited by Rapa/Lps in a concentration-dependent manner, and the inhibitory effect of Rapa/Lps was significantly stronger than that of free Rapa (Figure 5B). The IC_{50} was 14.67±2.57μg/mL in free Rapa and 5.18±3.52 μg/mL in Rapa/Lps. It showed that Rapa/Lps significantly enhanced its cytotoxicity to HUVECs compared with free Rapa. Moreover, Rapa/Lps enhances the cytotoxic effect of 5-FU on HUVEC cells (Figure 5C).

The Combination of Rapa/Lps and 5-FU Inhibit Tube Formation and Migration of HUVECs

Many studies have found the correlation between tumor growth and angiogenesis.[16,17] We suppose that the anti-cancer effect of Rapa/Lps was related to angiogenesis. As is shown in Figure 6A and D, HUVECs formed capillary-like structures in the control group. In contrast, Rapa/Lps significantly destroyed the tube formation of HUVECs. Vascular endothelial growth factor (VEGF) plays a crucial role in angiogenesis.[18] Therefore, we explored the drug's effect on

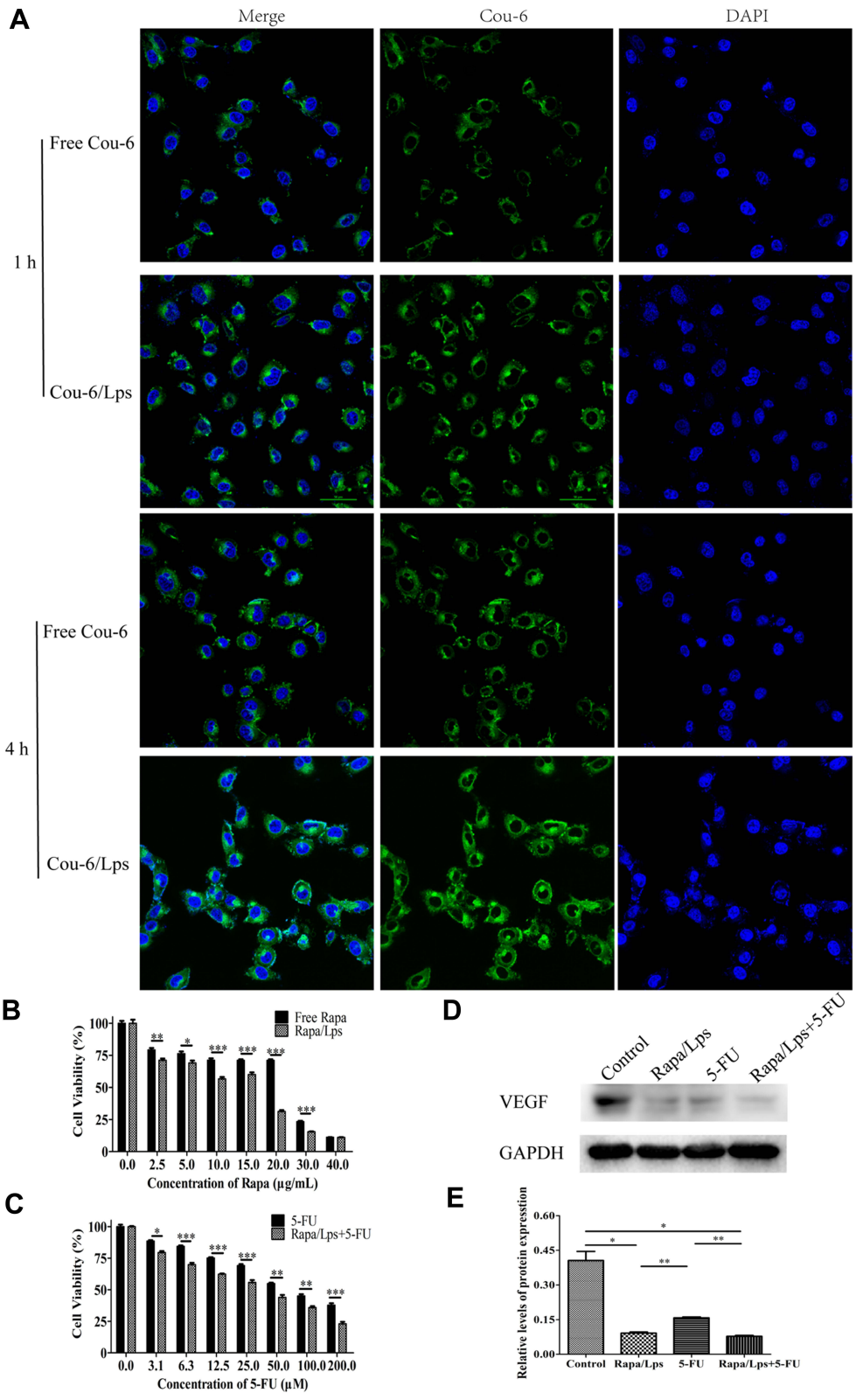

Figure 5 Cell uptake and proliferation of colorectal cancer cells treated by different drug groups. (**A**) Free coumarin-6 and coumarin-6 liposomes cellular uptake by HUVECs. (**B**) The cell viability of HUVECs after treatment free Rapa or Rapa/Lps for 48 hours. (**C**) The cell viability of HUVECs after treatment 5-FU or Rapa/Lps combined with 5-FU for 48 hours. (**D** and **E**) The VEGF protein expression in HUVECs was examined by Western blot analysis, and the protein levels were quantified by densitometry. Data are shown as mean ± SEM. $^{*}P < 0.05$, $^{**}P < 0.01$, $^{***}P < 0.001$.

https://doi.org/10.2147/IJN.S373777 DovePress

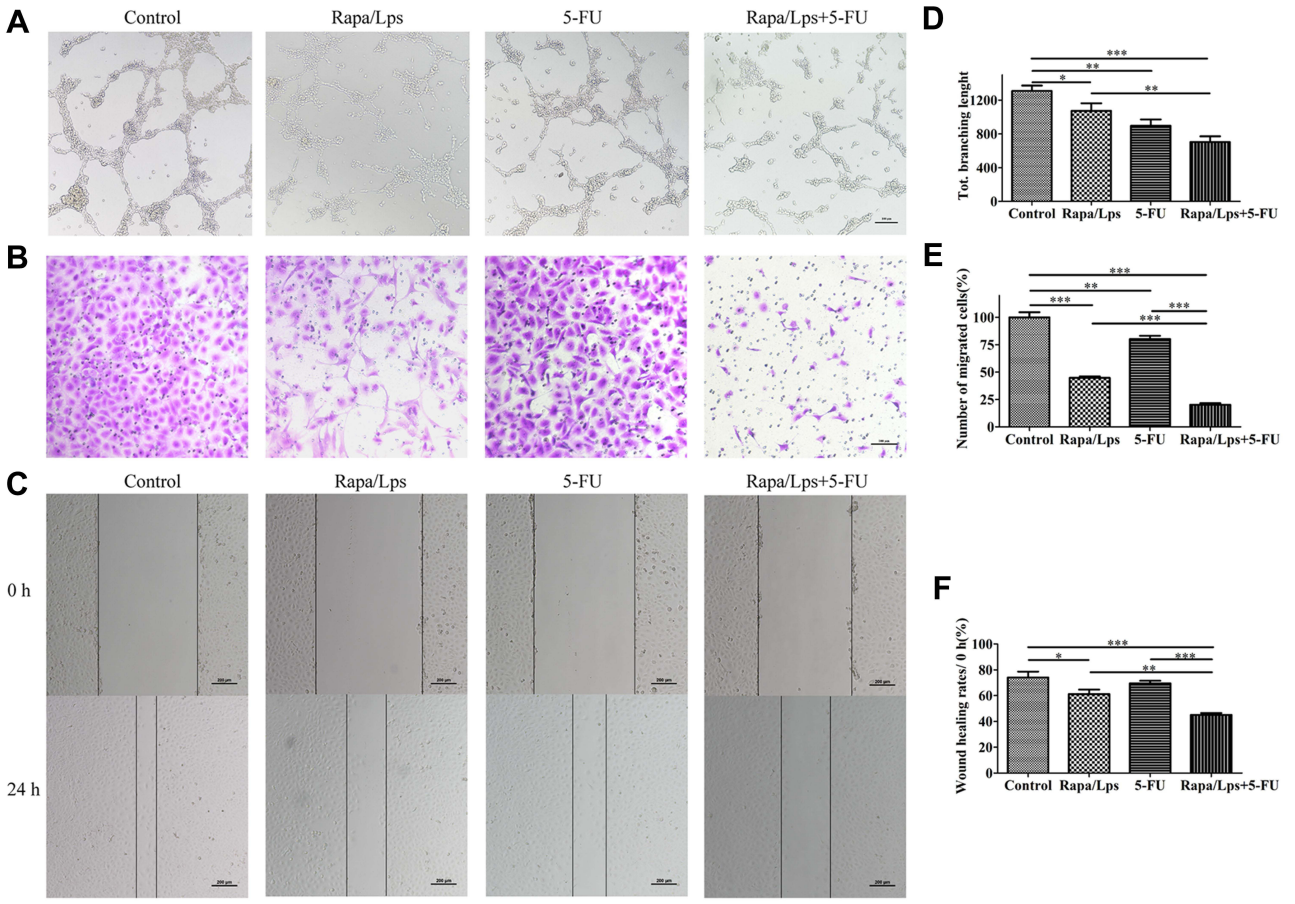

Figure 6 The combination of Rapamycin liposomes and 5-FU inhibit angiogenesis and migration in HUVECs. Representative images (**A**) and quantitative data (**D**) of the tube formation assay to assess the effect of drugs on HUVECs. Representative images (**B**) and quantitative data (**E**) of the transwell migration assay to assess the effect of drugs on HUVECs. Representative images (**C**) and quantitative data (**F**) of the wound healing assay to assess the effect of drugs on HUVECs. Data are shown as mean ± SEM (n=6). **P* < 0.05,***P* < 0.01, ****P* < 0.001.

VEGF protein level on HUVECs (Figure 5D and E), and co-treatmentRapa/Lps and 5-FU down-regulated the VEGF protein level in compared with control ($P<0.05$).

In addition, we also used wound healing assay and transwell assay to explore the effect on the migration ability of HUVECs. For the transwell assay (Figure 6B and E), the migration rate in Rapa/Lps (44.77 ± 2.17%, $P<0.001$), 5-FU (80.23 ± 5.00%, $P<0.01$,) and Rapa/Lps+5-FU (20.15 ± 2.94%, $P<0.001$) was significantly decreased. We also found similar results in the wound healing assay. The wound healing rate of the control group was 74.01±10.35% (Figure 6C and F). After drug treatment, the migration rate was 61.23 ± 4.86% in Rapa/Lps ($P<0.05$) and 69.53 ± 4.10% in 5-FU, which was further reduced to 45.16 ± 2.74% in the co-treatment group ($P<0.001$). These results enlighten the combination of Rapa/Lps and 5-FU may suppress the migration of HUVECs.

Discussion

APC was a tumor suppressor gene that also acted as a Wnt signaling pathway negative regulator. Early embryogenesis, stem cell maintenance, cell proliferation, and differentiation have all been associated with the highly conserved Wnt/-catenin signaling pathway.[19,20] APC truncating mutations activated the Wnt signaling pathway, which disrupted a variety of cellular processes.[21] The APC $^{(Min/+)}$ mice were used to study FAP. Rapamycin was found to prolong life in the APC$^{(Min/+)}$ colon cancer FAP model in a previous study.[22] Our study demonstrates the combination of Rapa/Lps and 5-FU dramatically decreased the number and load of tumors in APC $^{(Min/+)}$ mice. Furthermore, APC $^{(Min/+)}$ mice developed splenomegaly, which improved after drug treatment.

The combination of AOM with the pro-inflammatory reagent DSS is particularly useful for studying chronic colitis-driven tumor progression.[23] Previous research has found that AOM/DSS tumors are similar to human CRC in many ways, including tumor location, histopathological features, and molecular features.[4] We discovered the tumor load and max tumor size of Rapa/Lps+5-FU were reduced in AOM/DSS colorectal cancer mice, thus significantly inhibiting the formation of large-diameter tumors.

Tumors will secrete high levels of growth factors to establish an aberrant immature vascular network to meet the high proliferation rate of cancer cells, resulting in decreased tumor perfusion and higher metastatic dissemination risks.[24,25] Bevacizumab is the first anti-angiogenic drug that targets VEGF in the treatment of advanced metastatic colorectal cancer.[26] HUVECs and CD31 immunohistochemistry were used to explore the anti-cancer activity of Rapa/Lps coupled with 5-FU in this study.

HUVECs are vascular-like cells that are often employed in angiogenesis research[27,28] Our results revealed that treatments with Rapa/Lps or 5-FU, specifically Rapa/Lps+5-FU may considerably decrease the development of vascular structure in HUVECs. The downregulation of VEGF also supported the conclusion. Many studies have discovered that abnormal vascular causes excessive permeability, poor perfusion, and hypoxia, promoting cancer cell metastasis.[25] Sun et al[29] demonstrated that chalcone analogs 7 m effectively inhibited angiogenesis, metastasis, and proliferation in vitro and zebrafish xenografts. Interestingly, we observed synergistic treatment significantly suppressed the migration of HUEVCs. It enlightened the combination of Rapa/Lps and 5-FU could inhibit angiogenesis and metastasis. The low expression of CD31 and Ki67 in two mouse models also showed Rapa/Lps+5-FU magnificently suppressed the growth of the tumor by inhibiting micro-angiogenesis and tumor cell proliferation.

Furthermore, we also found Rapa/Lps was more cytotoxic to HUEVCs than free Rapa. Cellular uptake experiments revealed that Cou-6/Lps considerably increased intracellular green fluorescence intensity compared to free Cou-6. The improvement in cellular absorption might be related to a shift in the drug entry mechanism. Liposomes enter cells by electrostatic adsorption or endocytosis after encapsulation, and they have a slow-release activity, implying an increase in intracellular concentration.[30,31] Liposomes can encapsulate both hydrophobic and hydrophilic medicines, enhancing their solubility, stability, and tumor targeting while reducing negative effects on normal cells and tissue.[32] Our previous findings support this conclusion. DiR liposomes significantly increased drug enrichment at tumor sites compared to free DiR.[11] Indeed, liposomes further modify active targeting ligands that can improve tumor targeting.[33,34] Concerning the safety of liposomes, lipid-based colloidal carriers will typically be tolerated well in living systems since they are built from physiological compounds, and, therefore, metabolism should reduce toxicity.[35,36]

In summary, inhibiting tumor angiogenesis was an effective treatment with CRC, which blocked the nutrient supply and waste output, resulting in the inhibition of tumor growth, invasion, and metastasis.[17,29] However, recent research also demonstrated that over-inhibition of angiogenesis results in increased drug resistance of tumor cells and easier aggregation of tumor stem cells, thereby facilitating tumor invasion and metastasis.[37,38] Importantly, Rapa induces the death of tumor cells through various mechanisms, including apoptosis,[39] autophagy,[39,40] and ferroptosis.[41] In addition, early detection is crucial for improving the survival rate of CRC patients. Metadherin mRNA expression in serum has been shown in several studies to be a valuable non-invasive biomarker in the early detection of CRC as well as to augment the efficacy.[42,43] Furthermore, this study evaluated only Rapa/Lps in combination with 5-FU in mice, so human results would need to be confirmed before being applied clinically.

Conclusion

Rapa/Lps combined with 5-FU had a promising anti-tumor effect in APC $^{(Min/+)}$ and AOM/DSS colitis-induced colorectal cancer mice. Our research showed that the combination could suppress tumor growth by inhibiting angiogenesis and migration in vitro and in vivo, revealing the efficacy of Rapa/Lps+5-FU as a therapeutic strategy in colorectal cancer.

Acknowledgments

This work was supported by the National Natural Science Foundation of China (No. 81971742), the Natural Science Foundation of Guangdong Province (No. 2022A1515010199), Guangzhou Science and Technology Plan Project (202102020149) and Academician He Lin Scientific Research Fund (2021HLKY07).

Disclosure

The authors declare no conflicts of interest in this work.

References

1. Sung H, Ferlay J, Siegel RL, et al. Global cancer statistics 2020: GLOBOCAN estimates of incidence and mortality worldwide for 36 cancers in 185 countries. *CA Cancer J Clin*. 2021;71(3):209–249. doi:10.3322/caac.21660
2. Keller DS, Windsor A, Cohen R, Chand M. Colorectal cancer in inflammatory bowel disease: review of the evidence. *Tech Coloproctol*. 2019;23(1):3–13. doi:10.1007/s10151-019-1926-2
3. Koehl GE, Spitzner M, Ousingsawat J, Schreiber R, Geissler EK, Kunzelmann K. Rapamycin inhibits oncogenic intestinal ion channels and neoplasia in APC$^{(Min/+)}$ mice. *Oncogene*. 2010;29(10):1553–1560. doi:10.1038/onc.2009.435
4. Neufert C, Becker C, Neurath MF. An inducible mouse model of colon carcinogenesis for the analysis of sporadic and inflammation-driven tumor progression. *Nat Protoc*. 2007;2(8):1998–2004. doi:10.1038/nprot.2007.279
5. Yu T, Guo F, Yu Y, et al. Fusobacterium nucleatum promotes chemoresistance to colorectal cancer by modulating autophagy. *Cell*. 2017;170(3):548–563 e16. doi:10.1016/j.cell.2017.07.008
6. Sethy C, Kundu CN. 5-fluorouracil (5-FU) resistance and the new strategy to enhance the sensitivity against cancer: implication of DNA repair inhibition. *Biomed Pharmacother*. 2021;137:111285. doi:10.1016/j.biopha.2021.111285
7. Meng QY, Cong HL, Hu H, Xu FJ. Rational design and latest advances of codelivery systems for cancer therapy. *Mater Today Bio*. 2020;7:100056. doi:10.1016/j.mtbio.2020.100056
8. Prompipak J, Senawong T, Sripa B, et al. Anticancer effects of the combined Thai noni juice ethanolic extracts and 5-fluorouracil against cholangiocarcinoma cells in vitro and in vivo. *Sci Rep*. 2021;11(1):14866. doi:10.1038/s41598-021-94049-z
9. Sang J, Tang R, Yang M, Sun Q. Metformin inhibited proliferation and metastasis of colorectal cancer and presented a synergistic effect on 5-FU. *Biomed Res Int*. 2020;2020:9312149. doi:10.1155/2020/9312149
10. Coates A, Abraham S, Kaye SB, et al. On the receiving end--patient perception of the side-effects of cancer chemotherapy. *Eur J Cancer Clin Oncol*. 1983;19(2):203–208. doi:10.1016/0277-5379(83)90418-2
11. Chen YQ, Zhu WT, Lin CY, Yuan ZW, Li ZH, Yan PK. Delivery of rapamycin by liposomes synergistically enhances the chemotherapy effect of 5-fluorouracil on colorectal cancer. *Int J Nanomedicine*. 2021;16:269–281. doi:10.2147/IJN.S270939
12. Hutchinson L, Kirk R. High drug attrition rates--where are we going wrong? *Nat Rev Clin Oncol*. 2011;8(4):189–190. doi:10.1038/nrclinonc.2011.34
13. Liu M, Xie W, Wan X, Deng T. Clostridium butyricum modulates gut microbiota and reduces colitis associated colon cancer in mice. *Int Immunopharmacol*. 2020;88:106862. doi:10.1016/j.intimp.2020.106862
14. Khondee S, Rabinsky EF, Owens SR, et al. Targeted therapy of colorectal neoplasia with rapamycin in peptide-labeled pegylated octadecyl lithocholate micelles. *J Control Release*. 2015;199:114–121. doi:10.1016/j.jconrel.2014.11.034
15. Li Q, Chen C, Liu C, et al. The effects of cellulose on AOM/DSS-Treated C57BL/6 colorectal cancer mice by changing intestinal flora composition and inflammatory factors. *Nutr Cancer*. 2021;73(3):502–513. doi:10.1080/01635581.2020.1756355
16. Al-Ostoot FH, Salah S, Khamees HA, Khanum SA. Tumor angiogenesis: current challenges and therapeutic opportunities. *Cancer Treat Res Commun*. 2021;28:100422. doi:10.1016/j.ctarc.2021.100422
17. Teleanu RI, Chircov C, Grumezescu AM, Teleanu DM. Tumor angiogenesis and anti-angiogenic strategies for cancer treatment. *J Clin Med*. 2019;9(1):84. doi:10.3390/jcm9010084
18. De Palma M, Biziato D, Petrova TV. Microenvironmental regulation of tumour angiogenesis. *Nat Rev Cancer*. 2017;17(8):457–474. doi:10.1038/nrc.2017.51
19. Klaus A, Birchmeier W. Wnt signalling and its impact on development and cancer. *Nat Rev Cancer*. 2008;8(5):387–398. doi:10.1038/nrc2389
20. Steinhart Z, Angers S. Wnt signaling in development and tissue homeostasis. *Development*. 2018;145(11):146589. doi:10.1242/dev.146589
21. Zhang L, Shay JW. Multiple roles of APC and its therapeutic implications in colorectal cancer. *J Natl Cancer Inst*. 2017;109(8):djw332. doi:10.1093/jnci/djw332
22. Parihar M, Dodds SG, Hubbard G, et al. Rapamycin extends life span in Apc$^{(Min/+)}$ colon cancer FAP model. *Clin Colorectal Cancer*. 2021;20(1):e61–e70. doi:10.1016/j.clcc.2020.08.006
23. Ding L, Yang L, Wang Z, Huang W. Bile acid nuclear receptor FXR and digestive system diseases. *Acta Pharm Sin B*. 2015;5(2):135–144. doi:10.1016/j.apsb.2015.01.004
24. Viallard C, Larrivee B. Tumor angiogenesis and vascular normalization: alternative therapeutic targets. *Angiogenesis*. 2017;20(4):409–426. doi:10.1007/s10456-017-9562-9
25. Petrillo S, Tolosano E, Munaron L, Genova T. Targeting metabolism to counteract tumor angiogenesis: a review of patent literature. *Recent Pat Anticancer Drug Discov*. 2018;13(4):422–427. doi:10.2174/1574892813666180528105023
26. Ferrara N, Hillan KJ, Gerber HP, Novotny W. Discovery and development of bevacizumab, an anti-VEGF antibody for treating cancer. *Nat Rev Drug Discov*. 2004;3(5):391–400. doi:10.1038/nrd1381
27. Gentile MT, Pastorino O, Bifulco M, Colucci-D' Amato L. HUVEC tube-formation assay to evaluate the impact of natural products on angiogenesis. *J Vis Exp*. 2019;(148). doi:10.3791/58591
28. Zhao JY, Lin W, Zhuang QC, Zhong XY, Peng J, Hong ZF. Bear bile powder inhibits angiogenesis in vivo and in vitro. *Chin J Integr Med*. 2015;21(5):369–375. doi:10.1007/s11655-015-2062-0
29. Sun M, Wang Y, Yuan M, et al. Angiogenesis, anti-tumor, and anti-metastatic activity of novel alpha-substituted hetero-aromatic chalcone hybrids as inhibitors of microtubule polymerization. *Front Chem*. 2021;9:766201. doi:10.3389/fchem.2021.766201
30. Bozzuto G, Molinari A. Liposomes as nanomedical devices. *Int J Nanomedicine*. 2015;10:975–999. doi:10.2147/IJN.S68861
31. El Maghraby GM, Arafa MF. Liposomes for enhanced cellular uptake of anticancer agents. *Curr Drug Deliv*. 2020;17(10):861–873. doi:10.2174/1567201817666200708113131

32. Yingchoncharoen P, Kalinowski DS, Richardson DR. Lipid-based drug delivery systems in cancer therapy: what is available and what is yet to come. *Pharmacol Rev*. 2016;68(3):701–787. doi:10.1124/pr.115.012070
33. Yalikong A, Li XQ, Zhou PH, et al. A triptolide loaded HER2-targeted nano-drug delivery system significantly suppressed the proliferation of HER2-positive and BRAF mutant colon cancer. *Int J Nanomedicine*. 2021;16:2323–2335. doi:10.2147/IJN.S287732
34. Xu Y, Yao Y, Wang L, Chen H, Tan N. Hyaluronic acid coated liposomes co-delivery of natural cyclic peptide RA-XII and mitochondrial targeted photosensitizer for highly selective precise combined treatment of colon cancer. *Int J Nanomedicine*. 2021;16:4929–4942. doi:10.2147/IJN.S311577
35. Onoue S, Yamada S, Chan HK. Nanodrugs: pharmacokinetics and safety. *Int J Nanomedicine*. 2014;9:1025–1037. doi:10.2147/IJN.S38378
36. Martins S, Sarmento B, Ferreira DC, Souto EB. Lipid-based colloidal carriers for peptide and protein delivery--liposomes versus lipid nanoparticles. *Int J Nanomedicine*. 2007;2(4):595–607.
37. Lugano R, Ramachandran M, Dimberg A. Tumor angiogenesis: causes, consequences, challenges and opportunities. *Cell Mol Life Sci*. 2020;77(9):1745–1770. doi:10.1007/s00018-019-03351-7
38. Vasudev NS, Reynolds AR. Anti-angiogenic therapy for cancer: current progress, unresolved questions and future directions. *Angiogenesis*. 2014;17(3):471–494. doi:10.1007/s10456-014-9420-y
39. Feng H, Cheng X, Kuang J, et al. Apatinib-induced protective autophagy and apoptosis through the AKT-mTOR pathway in anaplastic thyroid cancer. *Cell Death Dis*. 2018;9(10):1030. doi:10.1038/s41419-018-1054-3
40. Cheong H, Lu C, Lindsten T, Thompson CB. Therapeutic targets in cancer cell metabolism and autophagy. *Nat Biotechnol*. 2012;30(7):671–678. doi:10.1038/nbt.2285
41. Tsai Y, Xia C, Sun Z. The inhibitory effect of 6-gingerol on ubiquitin-specific peptidase 14 enhances autophagy-dependent ferroptosis and anti-tumor in vivo and in vitro. *Front Pharmacol*. 2020;11:598555. doi:10.3389/fphar.2020.598555
42. Abdel Ghafar MT, Gharib F, Abdel-Salam S, et al. Role of serum Metadherin mRNA expression in the diagnosis and prediction of survival in patients with colorectal cancer. *Mol Biol Rep*. 2020;47(4):2509–2519. doi:10.1007/s11033-020-05334-5
43. Abdel Ghafar MT, Soliman NA. Metadherin (AEG-1/MTDH/LYRIC) expression: significance in malignancy and crucial role in colorectal cancer. *Adv Clin Chem*. 2022;106:235–280.